Molecular Structure and Large-Amplitude Bending Vibration of Carbon Suboxide as Studied by Electron-Diffraction and Spectroscopic Data

Yasuhiro Ohshima, Satoshi Yamamoto* and Kozo Kuchitsu

Department of Chemistry, Faculty of Science, The University of Tokyo, Bunkyo-ku, Tokyo 113, Japan

Ohshima, Y., Yamamoto, S. and Kuchitsu, K., 1988. Molecular Structure and Large-Amplitude Bending Vibration of Carbon Suboxide as Studied by Electron-Diffraction and Spectroscopic Data. – Acta Chem. Scand., Ser. A 42: 307–317.

The geometrical structure of carbon suboxide has been reinvestigated by electron diffraction. The r_g distances for the C=O and C=C bonds have been determined to be 1.164(2) Å and 1.286(4) Å, respectively, where the uncertainties represent estimated limits of error. Available spectroscopic data such as the energy-level intervals and the rotational constants have also been taken into the analysis of the large-amplitude CCC bending vibration using a model which allows the C=C bond lengths and the CCO bond angles to vary with the bending displacement, ϱ ($= 180° - \angle CCC$). The effective bending potential function determined for the vibrational ground state has a barrier of 27(16) cm^{-1} and a minimum at ϱ = 20(2)°. The bond lengths corresponding to the linear configuration, averaged over all the small-amplitude vibrations, are determined to be r_{CO}^{lin} = 1.1602(15) Å and r_{CC}^{lin} = 1.2761(12) Å. The present analysis shows that the C=C bonds are slightly stretched by the CCC bending, and the CCO angles are slightly bent in the direction of the CCC bending. This model has resolved the reported discrepancy between the observed rotational constant and that calculated using the structure derived from electron diffraction.

Dedicated to Professor Otto Bastiansen on his 70th birthday

Carbon suboxide is one of the best-known "floppy" molecules. It has a large-amplitude and very anharmonic degenerate CCC bending mode, ν_7. The structure of this molecule has been studied repeatedly both by experiment and theory, particularly in relation to this quasi-linearity.[1] Bastiansen and his coworkers[2] observed the shrinkages [3–5] and mean-square amplitudes of vibration for non-bonded pairs by electron diffraction and showed that the bending potential could not be harmonic. Their pioneer work was followed up by Morino and his coworkers;[6] their analysis of the electron-diffraction intensity on the basis of a large-amplitude model led to the suggestion that a small hump was likely to be present at the linear configuration. An analysis of the shrinkage effect was also made by Clark and Seip.[7]

A number of spectroscopic studies with high resolution[1,8] have since been made, and it has been shown that the ν_7 vibration gives an irregular series of energy levels, the first interval being only about 18 cm^{-1}.[8–10] These energy levels have been analyzed by use of various effective Hamiltonians to describe the bending motion.[9–12] The potential barrier is known to be only about 30 cm^{-1} in the ground state[9–12] but it depends significantly on the excitation of other small-amplitude modes.[9–12]

There still remain, however, two important problems with regard to the structure of carbon suboxide. First, the horizontal axis of the bending potential has to be defined more precisely in order to determine the bending angle correspond-

*Present address: Department of Astrophysics, Faculty of Science, Nagoya University, Chikusa-ku, Nagoya 464, Japan.

ing to the potential minimum and the potential wall with higher accuracy. The angle coordinate depends on the effective mass of the ν_7 mode, which varies widely with degree of coupling between the CCC bending and other small-amplitude motions, especially the CCO bending.This coupling has been included effectively in the "semirigid bender Hamiltonian" set up by Bunker,[12] but all the available spectroscopic data seem still to be insufficient for estimating the degree of this coupling. A similar problem was encountered for cyclobutane, where the potential for the large-amplitude ring-puckering motion was determined by estimating the degree of coupling of this motion with other small-amplitude motions such as the CH_2 rocking;[13] in this case a joint analysis of electron-diffraction and spectroscopic data provided crucial information on the mode coupling. Thus, it was thought worthwhile to undertake a joint analysis of all the spectroscopic and electron-diffraction data for carbon suboxide to derive further information on the bending potential and the intermode coupling.

The second unsolved problem is the discrepancy between the rotational constant determined by high-resolution spectroscopy and that estimated from the structure derived from electron diffraction. As reported by Tanimoto *et al.*,[6] the B_z constant derived from the B_0 constant, 0.07330 cm^{-1}, disagreed significantly with the B_α^0 constant, 0.0738(2) cm^{-1}, estimated from the r_g bond lengths; the B_z and B_α^0 constants should normally agree much more closely.[14] Even the subsequent recalculation of these rotational constants by Duckett *et al.*[9] with careful consideration of the large-amplitude ν_7 motion could not remove this discrepancy. One should note, however, that their estimates[6,9] of B_α^0 were based on the neglect of the changes in the C=C and C=O bond lengths when the molecule was bent. As suggested by our recent study[15] for allene, this neglect would not necessarily be valid, e.g. for a molecule with multiple bonds, and a significant discrepancy between B_z and B_α^0 may result from the neglect of coupling between the bending and bond-stretching motions, particularly in a large-amplitude case. Therefore, a further analysis was made in the present study using a model in which this coupling was explicitly taken into account.

Experimental

The sample of C_3O_2 was prepared by dehydration of malonic acid using a mixture of silica and P_2O_5,[16] and purified by vacuum distillation. A small impurity of acetic acid (< 1%) was detected by a low-resolution IR spectrum upon comparison with the spectrum reported by Miller and Fateley.[17] It was possible to store the sample in a glass container at dry-ice temperature for more than a month without perceptible decomposition or polymerization.

Diffraction photographs were taken on Kodak Image plates by an apparatus equipped with an

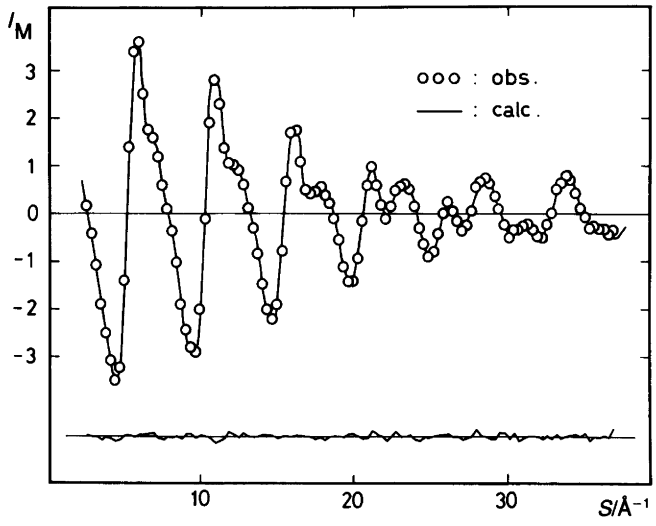

Fig. 1. Molecular intensity for C_3O_2. Observed values are shown as open circles, and the solid curve represents the best-fit theoretical intensity. The lower solid curve represents the residual.

r^3-sector.[18] The accelerating voltage of the electron beam, about 40 kV, was stabilized to within 0.01 % during the exposure, and the electron beam current was about 0.65 μA. The sample holder was cooled in a dry ice-ethanol bath (about −50 °C) in order to adjust the sample pressure (about 50 Torr) and condense the acetic acid impurity. Diffraction photographs were taken at about 23 °C (nozzle tip) with two camera lengths of 243.20 and 107.77 mm, and with exposure times of 25 and 40 s, respectively. The electron wavelength was calibrated with reference to the r_a (C=O) distance of carbon dioxide.[19] Molecular intensities ranging s = 6.3–37.4 Å^{-1} and 2.5–18.8 Å^{-1} were obtained from the data recorded with the short and long camera lengths, respectively.[6] Since these intensities were consistent within the range of experimental error, they were jointed at s = 13.2 Å^{-1}. A typical molecular intensity and the corresponding radial distribution curve are shown in Figs. 1 and 2, respectively.

Analysis

Preliminary analysis of electron-diffraction intensity. All the bonded or non-bonded internuclear distances, six in total, were taken as independent parameters, because the effect of the large-amplitude anharmonic bending vibration was so extensive that ordinary shrinkage corrections, r_a–r_α^0, for the non-bonded pairs based on the small-amplitude approximation[14,20] could not be adopted. Therefore, these six distances and the corrresponding mean amplitudes were varied in the least-squares refinement of the molecular intensity. The peaks for the non-bonded pairs in the radial distribution curve shown in Fig. 2, especially that for the $O_1 \cdots O_5$ distance, are skewed because of the ν_7 motion.[2,6] This distortion can be treated by introducing an asymmetry parameter, $\varkappa$, in the molecular intensity as $\sin[s(r_a - \varkappa s^2)]$.[21] Though the $\varkappa$ parameters for non-bonded pairs are often ignored for a molecule with small-amplitude vibrations only,[20] the neglect of the $\varkappa$ parameters in the present analysis introduces a serious systematic error. Hence, the $\varkappa$ parameters for the non-bonded pairs were introduced, but were fixed at the values calculated by a numerical method[13] considering the ν_7 motion, as described in the Appendix. Those for the bonded pairs were estimated from the anharmonic constants for the corresponding diatomic molecules, C_2 and CO.[22] The results are listed in Tables 1 and 2. The corresponding correlation matrix is given in Tabel 3. The r_g distance is related to r_a according to:[21]

$$r_g = r_a + l^2/r_a. \tag{1}$$

The shrinkages, δ_g for the non-bonded pairs[5] are listed in Table 4. The observed values of the shrinkages and the mean amplitudes for the non-bonded pairs agree within experimental error with those reported previously.[2,6]

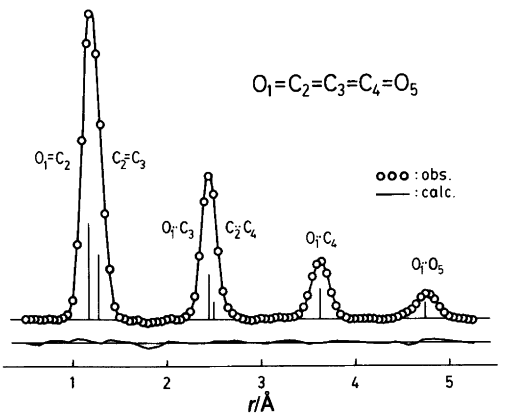

Fig. 2. Radial distribution curve for C_3O_2. Experimental values are shown as open circles, and the solid curve represents the best-fit theoretical values. A damping factor, exp ($-0.0020s^2$), is used. The lower solid curve represents the residual.

Hamiltonian for the large-amplitude bending motion. The following large-amplitude analysis of the ν_7 vibration was based on the effective Hamiltonian for the bending vibration derived by Bunker.[12] The semirigid-bender Hamiltonian, which describes approximately the rotation-bending motion for this molecule, is composed of three terms:[12]

$$H_{srb} = H_\varrho + H_{rot}^z + H_{rot}^{xy}, \tag{2}$$

$$H_\varrho = \tfrac{1}{2}\mu_{\varrho\varrho}J_\varrho^2 + \tfrac{1}{2}[J_\varrho,\mu_{\varrho\varrho}]J_\varrho + \tfrac{1}{2}\mu^{1/4}[J_\varrho,\mu_{\varrho\varrho}\mu^{-1/2}[J_\varrho,\mu^{1/4}]] + V_{gs}(\varrho), \tag{3}$$

$$H_{rot}^z = \tfrac{1}{2}\mu_{zz}J_z^2, \tag{4}$$

$$H_{rot}^{xy} = \tfrac{1}{2}\mu_{xx}J_x^2 + \tfrac{1}{2}\mu_{yy}J_y^2, \tag{5}$$

Table 1. Internuclear distances and asymmetry parameters for C_3O_2.[a]

	r_a/Å[b]	r_g/Å[b,c]	r_g/Å[d]	$\varkappa/10^{-7}$Å^3 [e]
$O_1=C_2$	1.1626(14)	1.1640(15)	1.1632(13)	7
$C_2=C_3$	1.284(4)	1.286(4)	1.289(2)	10
$O_1\cdots C_3$	2.442(14)	2.443(14)	2.445(5)	0
$C_2\cdots C_4$	2.49(4)	2.49(4)	2.485(17)	−70
$O_1\cdots C_4$	3.624(7)	3.626(7)	3.631(5)	−292
$O_1\cdots O_5$	4.742(18)	4.744(18)	4.755(13)	−1362

[a]Estimated limits of error in the last significant digits are given in parentheses. [b]Determined by electron diffraction in the present study. [c]Obtained by using eqn. (1). [d]Ref. 6. [e]Calculated from the parameters listed in Table 7 by the method described in the Appendix.

Table 2. Observed and calculated mean amplitudes for C_3O_2.

	l_{obs}/Å[a]			l_{calc}/Å	
	Ref. 2	Ref. 6	This work	I[b]	II[c]
$O_1=C_2$	0.039(8)	0.0368(13)	0.040(9)	0.0349	0.0349
$C_2=C_3$	0.043(11)	0.041(2)	0.046(10)	0.0387	0.0387
$O_1\cdots C_3$	0.0470	0.042(2)	0.045(9)	0.0419	0.0420
$C_2\cdots C_4$	0.0650	0.076(19)	0.07(5)	0.0673	0.0581
$O_1\cdots C_4$	0.08(3)	0.081(7)	0.078(6)	0.0819	0.0745
$O_1\cdots O_5$	0.11(11)	0.099(10)	0.099(19)	0.1100	0.1072
T/K[d]	290	293	296		

[a]Estimated limits of error in the last significant digits are given in parentheses. [b]Calculated by a large-amplitude analysis assuming $X_\tau = 0$, as described in the Appendix. The parameters used are taken from Ref. 12. [c]Calculated by a large-amplitude analysis assuming $X_\tau = -0.10$ (best fit), as described in the Appendix. The parameters used are listed in Table 7. [d]Approximate temperature at the nozzle tip.

where

$$\mu = \mu_{xx}\mu_{yy}\mu_{zz}\mu_{\varrho\varrho}. \quad (6)$$

V_{gs} (ϱ) is the effective bending potential for the ground-state manifold. The reciprocal moment of inertia around the α-axis is represented by $\mu_{\alpha\alpha}$ ($\alpha = x, y, z$), and $\mu_{\varrho\varrho}$ is the reciprocal reduced mass for the bending vibration, i.e.:

$$\mu_{\varrho\varrho} = 1/\sum_i m_i[(dy_i/d\varrho)^2 + (dz_i/d\varrho)^2], \quad (7)$$

The molecule-fixed axes and the bending coordinate, ϱ, are defined in Fig. 3; J_x, J_y and J_z are the components of the total angular momentum, and J_ϱ is the momentum conjugate with ϱ, $J_\varrho = -i\hbar d/d\varrho$.

The bond lengths, r_{CO} and r_{CC}, and the CCO angles, τ, are assumed to depend on the ϱ coordinate according to:[12]

$$r_{CO} = r_{CO}^{lin} + Y_{CO}\varrho^2, \quad (8)$$

$$r_{CC} = r_{CC}^{lin} + Y_{CC}\varrho^2, \quad (9)$$

$$\tau = X_\tau\varrho, \quad (10)$$

where Y_{CO}, Y_{CC}, and X_τ represent the mixing between the CCC bending and other vibrational modes; they are related to the second- and third-order force constants, as discussed in the following section. The sign of τ is defined in Fig. 3. The bending-potential function is modelled as

$$V_{gs}(\varrho) = f_2\varrho^2 + f_4\varrho^4, \quad (11)$$

Table 3. Correlation Matrix (× 100) for C_3O_2.[a]

	k_1	k_2	x_1	x_2	x_3	x_4	x_5	x_6	l_1	l_2	l_3	l_4	l_5	l_6
k_1	100	54	8	39	26	−17	0	−1	56	52	31	33	21	9
k_2		100	2	47	30	−21	−2	−3	82	68	52	40	27	11
x_1			100	49	4	−3	0	0	5	15	4	4	1	1
x_2				100	17	−13	−1	−1	31	29	26	22	14	6
x_3					100	−90	−1	−1	26	23	59	95	9	4
x_4						100	0	1	−19	−17	−72	−83	−6	−3
x_5							100	−1	−1	−1	−1	−1	−2	1
x_6								100	−2	−2	−2	−1	−1	−2
l_1									100	88	45	34	23	9
l_2										100	39	29	20	8
l_3											100	53	14	6
l_4												100	12	5
l_5													100	3
l_6														100

[a] k_1, k_2 = indices of resolution for data taken with the long and short camera lengths [0.99(2) and 0.94(5)], respectively;
$x_1 = r(O_1{=}C_2)$, $x_2 = r(C_2{=}C_3)$, $x_3 = r(O_1{\cdots}C_3)$, $x_4 = r(C_2{\cdots}C_4)$, $x_5 = r(O_1{\cdots}C_4)$, $x_6 = r(O_1{\cdots}O_5)$,
$l_1 = l(O_1{=}C_2)$, $l_2 = l(C_2{=}C_3)$, $l_3 = l(O_1{\cdots}C_3)$, $l_4 = l(C_2{\cdots}C_4)$, $l_5 = l(O_1{\cdots}C_4)$, $l_6 = l(O_1{\cdots}O_5)$.

Table 4. Observed and calculated shrinkages for C_3O_2.

	δ_g^{obs}/Å[a]			δ_g^{calc}/Å	
	Ref. 2	Ref. 6	This work	I[b]	II[c]
$O_1{\cdots}C_3$	(0.001)	0.008(6)	0.006(15)	0.0059	0.0066
$C_2{\cdots}C_4$	(0.140)	0.094(17)	0.08(5)	0.0882	0.0724
$O_1{\cdots}C_4$	0.110	0.111(6)	0.109(9)	0.1188	0.1081
$O_1{\cdots}O_5$	0.157	0.150(14)	0.156(19)	0.1725	0.1714
T/K[d]	290	293	296		

[a] Estimated limits of error in the last significant digits are given in parentheses. [b] Calculated by a large-amplitude analysis assuming $X_\tau = 0$, as described in the Appendix. The parameters used are taken from Ref. 12. [c] Calculated by a large-amplitude analysis assuming $X_\tau = -0.10$ (best fit), as described in the Appendix. The parameters used are listed in Table 7. [d] Approximate temperature at the nozzle tip.

The Hamiltonian for a non-rotating molecule exerting a bending motion can be represented after elimination of the end-over-end rotation term, H_{rot}^{xy}, as

$$H_{srb}^0 = H_\varrho + H_{rot}^z. \tag{12}$$

The eigenvalue, E_{vl}^0, and the eigenfunction, ψ_{vl}^0, for the v^l state can be obtained by numerical integration[23] using Cooley's method.[24] The energy level intervals and the rotational constant for each bending state determined experimentally by spectroscopy were fitted by this Hamiltonian to determine the bending-potential function, as described in the following section.

On the other hand, the structure derived from electron diffraction corresponds to the thermal average over vibration and rotation. Thus, the effective bending Hamiltonian averaged over rotation was used in the fitting of the electron-diffraction data. The end-over-end rotational term is approximately represented as

$$H_{rot}^{xy} \sim \tfrac{1}{4}(\mu_{xx} + \mu_{yy})(J_x^2 + J_y^2), \tag{13}$$

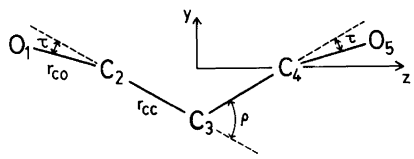

Fig. 3. The definition of coordinate system and internal coordinates of C_3O_2 used in the present large-amplitude analysis. The value of τ is positive when the CCO angles are in the opposite direction to the CCC angle.

by assuming that the difference between μ_{xx} and μ_{yy} is negligible. After thermal averaging of the total angular momentum at temperature T, denoted as $< >_T$, the H^{xy}_{rot}term is given by

$$<H^{xy}_{\text{rot}}>_T = \frac{1}{2}\left(\mu_{xx} + \mu_{yy}\right)\frac{hkT}{8\pi^2 cB} \equiv V_{\text{cent}}(\varrho), \tag{14}$$

where B denotes the rotational constant. Since this term can be regarded as the centrifugal correction for the bending-potential function, it is hereafter denoted as $V_{\text{cent}}(\varrho)$. The effective Hamiltonian corresponding to the thermal average over rotation is thus constructed by

$$H'_{\text{srb}} = H^0_{\text{srb}} + V_{\text{cent}}(\varrho) = H_\varrho + H^z_{\text{rot}} + V_{\text{cent}}(\varrho). \tag{15}$$

The eigenvalue, E'_{vl}, and the eigenfunction, ψ'_{vl}, for H'_{srb} were obtained in the same way as those for H^0_{srb}.

Shrinkage effect and bending-bending coupling. The shrinkages and the mean amplitudes were calculated as described in the Appendix by using the bending-potential function taken from Ref. 12, where the fitting of the observed vibrational energy levels[10] was initially based on the assumption that X_τ was zero. The agreement between the observed and calculated values was fair except that the calculated values for the $O_1\cdots C_4$ and $O_1\cdots O_5$ pairs were larger than the observed values, as shown in Tables 2 and 4. We interpreted the origin of these discrepancies as being that the C=C=O bonds were assumed to remain co-linear as the CCC angle was bent. In other words, the X_τ constant is expected to be *negative*; the reduced mass for the bending vibration then increases as $|X_\tau|$ increases, and the mean amplitude of the CCC bending is largely dehanced. The sum of squares of the residuals in the shrinkages is plotted against X_τ in Fig. 4. This plot indicates that X_τ can be estimated using the shrinkages observed by electron diffraction.

Rotational constants and bending-stretching coupling. The rotational constants determined by high-resolution spectroscopy were also used as valuable information on the molecular structure. For this purpose, the influence of the large-amplitude and small-amplitude vibrations on the average structure was treated as follows. Since excitation of the ν_7 bending vibration was known to cause an irregular change in the rotational constants of C_3O_2,[10] as shown in Table 5, the rotational constant for the v^l state, B_{vl}, was fitted by the following expression:[25]

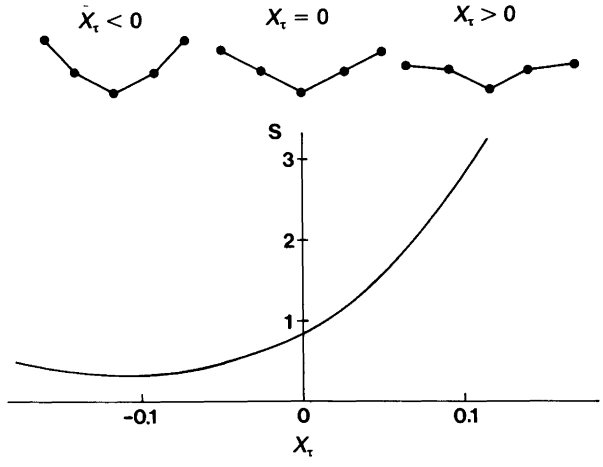

Fig. 4. A plot of the sum, S, of squares of the residuals in the shrinkages, δ_g, against the bending-bending coupling parameter, X_τ.

Table 5. Dependence of rotational constants on excitation of the ν_7 mode for C_3O_2.

$v_7^{l_7}$	B_{obs}/cm^{-1} [a]	$\Delta/10^{-6}$ cm^{-1} [b]
0^0	0.075564	14
1^1	0.076311	3
2^2	0.076941	0
2^0	0.076260	−20
3^3	0.077509	−1
3^1	0.076948	−5
4^2	0.077557	5
4^0	0.077291	−5
5^1	0.077793	4
6^2	0.078296	4
B_0^*/cm^{-1} [c]	0.073652(24)	
α_0/cm^{-1} [c]	0.01886(25)	
β_0/cm^{-1} [c]	0.00355(50)	

[a]From Table 1 of Ref. 10. [b]$\Delta = B_{obs} - B_{calc}$; B_{calc} is calculated using eqn. (16). [c]Parameters are defined in eqn. (16). One standard deviation in the last significant digit is given in parentheses.

$$B_{vl} = B_0^* + \alpha_0 \langle \varrho^2 \rangle_{vl} + \beta_0 \langle \varrho^4 \rangle_{vl}, \qquad (16)$$

where $\langle \ \rangle_{vl}$ denotes the vibrational average for the v^l state calculated from the eigenfunction ψ_{vl}^0 for the Hamiltonian given in eqn. (12). The value of B_0^* represents the effective rotational constant in the linear reference configuration, $\varrho = 0$. The rotational constant B_z^*, which corresponds to the linear configuration averaged over the small-amplitude modes, can be calculated by[9]

$$B_z^* = B_0^* + \sum_{s \neq 7} \alpha_s(\text{harm})\, d_s/2, \qquad (17)$$

where the degeneracy of the s-th mode is denoted as d_s. The harmonic force constants were taken from Ref. 9. This B_z^* constant was also calculated from the r_α^0 structure determined by electron diffraction. The r_α^0(C=C) and r_α^0(C=O) distances were obtained from the r_a(C=C) and r_a(C=O) distances by using the r_a–r_α^0 correction terms calculated with the aid of the diatomic approximation,[20,22] where the ν_7 mode was left out. The rotational constant calculated from the r_α^0(C=C) and r_α^0(C=O) distances was smaller than the B_z^* constant from the experimental rotational constants, as shown in Table 6. The discrepancy,

Table 6. Observed and calculated rotational constants for C_3O_2.

	SP[b]	ED (Y_{CC}=0)[c]	ED[d]
B_z^*/cm^{-1} [a]	0.07363(3)	0.07318(6)	0.07363(2)

[a]Rotational constant corresponding to the linear configuration. One standard deviation in the last significant digit is given in parentheses. [b]Obtained from B_0^* in Table 5 by using eqn. 17. [c]Calculated from the results of the preliminary analysis assuming $Y_{CC} = 0$. [d]Calculated from the final results listed in Table 7.

0.00045 cm^{-1}, was much larger than the experimental uncertainty, as pointed out in Refs. 6 and 9. We explained the origin of this discrepancy in terms of the coupling of the CCC bending motion with the bond-stretching motion.[12,15] If the bond distances are stretched as the CCC angle is bent, the bond distances averaged over the bending vibration are *increased* by comparison with those in the linear configuration, as shown schematically in Fig. 5. The magnitude of the coupling between the CCC bending and the bond-stretching was estimated by the following least-squares analysis.

Simultaneous analysis of electron-diffraction and spectroscopic data. The molecular structure, the

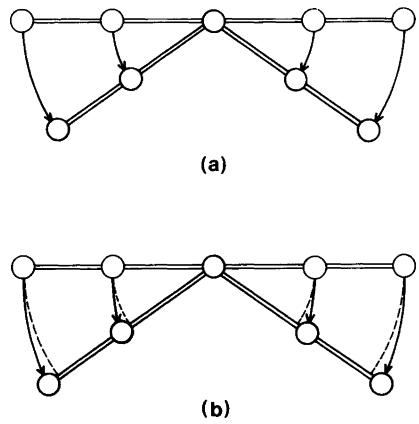

Fig. 5. Loci of the atoms in the CCC bending vibration of C_3O_2: (a) bending-stretching coupling is ignored; (b) a positive bending-stretching parameter, Y_{CC}, is included.

bending-potential function, and the parameters representing the bending-bending and bending-stretching couplings were determined in this stage by a joint analysis of the electron-diffraction intensity and the spectroscopic data. The energy levels calculated by using eqn. (12), the molecular intensity calculated from the eigenvalues and eigenfunctions for H'_{srb} in eqn. (15) (see Appendix), and the rotational constant, B_z^*, obtained from the r_{CC}^{lin} and r_{CO}^{lin} distances were compared with the corresponding experimental values in a least-squares refinement. The r_{CC}^{lin}, r_{CO}^{lin}, f_2, f_4, X_τ, and Y_{CC} parameters were varied in the refinement, but the Y_{CO} parameter had to be ignored because only one bending-stretching coupling parameter could be determined from the available data; Y_{CC} was chosen as an independent variable parameter because the C=C distances were expected to be more sensitive to the CCC bending than the C=O distances. The determined parameters are listed in Table 7. The calculated energy levels and the B_z^* constant are shown in Tables 8 and 6, respectively. The fitting of the rotational constants was repeated with the eigenfunctions calculated from the determined parameters, but the results were essentially unchanged. When Y_{CO} was assumed to be ± 0.010 Å rad^{-2}, the changes in r_{CC}^{lin}, r_{CO}^{lin} and Y_{CC} were ± 0.0015 Å, ∓ 0.0020 Å, and ∓ 0.007 Å rad^{-2}, respectively, and those in the other parameters were much smaller than the standard deviations in the refinement. These values were estimated to be the limits of the systematic error originating from the uncertainty in Y_{CO}. The mean amplitudes and the shrinkages for the non-bonded pairs calculated by using the final parameters were consistent with the observed values within the estimated limits of uncertainty, as shown in Tables 2 and 4.

Table 7. Best-fit parameters obtained in the large-amplitude analysis.[a]

f_2/cm^{-1} rad^{-2}	−449(25)
f_4/cm^{-1} rad^{-4}	1887(215)
r_{CC}^{lin}/Å	1.2761(4)
r_{CC}^{lin}/Å	1.1602(5)
Y_{CC}/Å rad^{-2}	0.022(3)
Y_{CO}/Å rad^{-2}	0.0[b]
X_τ	−0.10(3)
ϱ_e/°	19.7(8)
H/cm^{-1}	26.6(55)

[a]One standard deviation in the last significant digit is given in parentheses. The systematic error originating from the uncertainty in Y_{CO} is not included. See text for details. [b]Fixed in the least-squares refinement.

Table 8. Observed and calculated ν_7 vibrational energy levels.

$v_7^{l_7}$	E_{obs}^0/cm^{-1} [a]	Δ/cm^{-1} [b]
0^0	(0.0)	(0.0)
1^1	18.2558	−0.1301
2^2	46.1055	0.0485
2^0	60.7022	0.4222
3^3	80.65	0.39
3^1	97.2171	0.0781
4^4	120.52	0.88
4^2	137.2589	−0.1946
4^0	144.2985	−0.2590
5^5	164.55	1.15
5^3	181.10	−0.36
5^1	191.19	−0.78
6^6	212.51	1.53
6^4	229.83	0.91
6^2	239.56	−1.67
6^0	244.7	−1.0

[a]From Table 1 of Ref. 10. [b]$\Delta = E_{obs}^0 - E_{calc}^0$; E_{calc}^0 is calculated from the best-fit parameters listed in Table 7.

Discussion

Comparison of the geometrical structure. The r_g distances determined in the present study are in good agreement with those reported by Tanimoto *et al.*,[6] as shown in Table 1, and are also consistent with the r_a distances reported by Alemmingen *et al.*[2] within experimental uncertainties. These distances are compared in Table 9 with those for related molecules. The C=C distance is much shorter than those in ethylene,[26] allene[15] and ketene.[27] The C=O distance is also significantly shorter than that in formaldehyde[28] but is essentially equal to those in carbon dioxide[19] and ketene.[27] The latter trend corresponds to that in the force constants for the C=O stretching; the value for formaldehyde (12.9 aJ Å^{-2})[29] is much smaller than those for carbon dioxide (16.1 aJ Å^{-2}),[30] ketene (16.6 aJ Å^{-2})[31] and carbon suboxide (15.7 aJ Å^{-2}).[9]

Table 9. C=C and C=O bond distances in C_3O_2 and related molecules.[a]

Molecule	r_g(C=C)/Å	r_g(C=O)/Å	Ref.
O=C=C=C=O	1.286(4)	1.1640(15)	This work
O=C=O	–	1.16525(5)	19
H_2C=C=O	1.318(3)	1.166(2)	27
H_2C=C=CH_2	1.3129(9)	–	15
H_2C=O	–	1.209(2)	28
H_2C=CH_2	1.337(5)	–	26

[a]Estimated limits of error in the last significant digit are given in parentheses.

The C=O and C=C distances corresponding to the linear configuration, r^{lin}, have also been determined by a joint analysis of the electron-diffraction intensity and the rotational constant, B_z^*. The difference between r^{lin}, listed in Table 7, and r_g for the C=C bond (Δr = 0.010 Å) is much larger than that for the C=O bond (Δr = 0.004 Å); this difference is ascribed to the effect of the bending-stretching coupling as discussed below. The bond distances derived from an *ab initio* calculation using a (9*s*5*p*1*d*) basis set,[32] r(C=O) = 1.131 Å and r(C=C) = 1.266 Å, may be contrasted with the experimental r^{lin} values, 1.160 and 1.276 Å, respectively.

Potential function. The potential function for the ν_7 bending vibration, calculated from the values of f_2 and f_4 obtained in the present study, is compared in Fig. 6 with that derived by Bunker[12] under the assumption that $X_\tau = 0$. The barrier to linearity, H, remains essentially unchanged [26.6 (55) cm^{-1} for $X_\tau = -0.10$ and 28.08 cm^{-1} for X_τ = 0], but the horizontal axis of the potential curve is significantly different; the equilibrium ϱ value, ϱ_e, estimated in the present study is smaller than that reported by Bunker [19.7(8)° for $X_\tau = -0.10$ and 22.04° for X_τ = 0]. This is because the reduced mass for the bending vibration depends significantly on the X_τ constant. The reduced mass can hardly be determined from spectroscopic data only, because they do not provide sufficient information on the vibrational coupling, and hence the amplitude of the bending motion has to be left uncertain.

Electron diffraction provides quantitative information on the bending amplitude in the form of the shrinkages and the mean vibrational amplitudes. It has thus been possible to determine the potential function and the effective constants for coupling between the CCC-bending and CCO-bending modes in the present joint analysis of electron-diffraction and spectroscopic data.

In the present analysis the influence of overall rotation on the molecular structure is included in the large-amplitude bending Hamiltonian given in eqn. (15). This procedure takes account of the correction for centrifugal distortion needed for an analysis of electron diffraction by taking the thermal average of the structure over vibration and rotation. The V_{cent} term in eqn. (15) is very small for a semirigid molecule, but this correction cannot be ignored for C_3O_2. If the shrinkages for

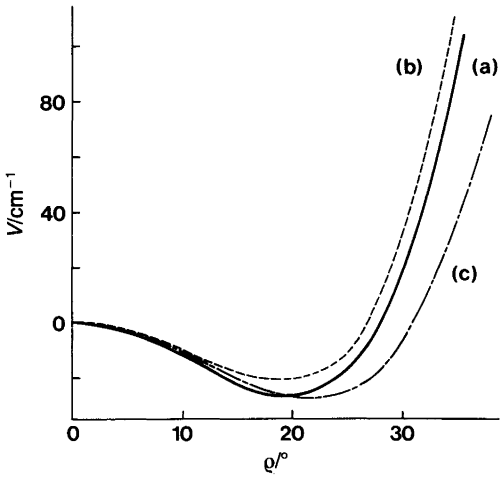

Fig. 6. Effective potential function for the CCC bending vibration of C_3O_2: (a) the best-fit potential for the ground state, V_{gs}, determined in the present study; (b) an effective potential in a rotating molecule at room temperature, where the centrifugal effect, V_{cent}, is included [see eqn.(15)]; (c) the potential for the ground state obtained by Bunker,[12] assuming $X_\tau = 0$.

the $O_1\cdots C_4$ and $O_1\cdots O_5$ distances are calculated without this centrifugal correction, the deviations from the corresponding observed values, 0.003 and 0.005 Å respectively, exceed experimental uncertainties.

Interaction between large-amplitude bending and other modes. The present joint analysis of electron-diffraction and spectroscopic data shows that the CCO angles are bent slightly in the direction of the CCC bending. No other experimental information on this type of coupling seems to have been reported except that the CCC angle in propadienone, $H_2C{=}C{=}C{=}O$, is 145° and the CCO angle is 169° in the opposite direction in the r_0 structure of this molecule.[33]

The bonds in carbon suboxide are found to be lengthened as the CCC angle is bent. This trend is consistent with those observed for CO_2,[30] CS_2,[34] and $CH_2{=}C{=}CH_2$.[15] The Y_{CC} constant, which effectively represents the coupling of the CCC bending with the C=C stretching, is approximately related to the second- and third-order force constants according to[12]

$$Y_{CC} = -\frac{F_{277}}{2\sqrt{2}F_{22}}, \tag{18}$$

where the subscripts 2 and 7 denote the symmetry coordinates S_2 and S_7, respectively. Using the harmonic force constant derived in Ref. 9, we obtain $F_{277} = -0.79(11)$ aJ Å^{-1} rad^{-2}. From this value, the third-order constant representing the mixing between the CCC bending and the C=C stretching, $f_{R\alpha\alpha}$, is estimated to be $-0.28(4)$ aJ Å^{-1} rad^{-2}. The sign and the order of magnitude of this constant are the same as those of the corresponding constants for CO_2, -0.588 aJ Å^{-1} rad^{-2},[30] CS_2, -0.370 aJ Å^{-1} rad^{-2},[34] and C_3H_4, -0.3 aJ Å^{-1} rad^{-2}.[15] However, the vibrationally averaged C=C bond lengths in C_3O_2 exceed those at $\varrho = 0$ by as much as 0.005 Å on account of the large amplitude of the CCC bending motion, whereas the corresponding difference in a semirigid molecule such as CO_2, CS_2 or C_3H_4 is smaller by one order of magnitude.

The third-order coupling among the vibrational modes in a semirigid molecule can be estimated by a joint analysis of electron-diffraction intensity and the rotational constants, including those for the bending excited states, as pointed out in our recent study on allene.[15] The present study aims to extend such an analysis to a quasi-linear molecule. In the light of the coupling between the large-amplitude and small-amplitude modes, the reported discrepancy[6,9] between the rotational constant obtained from spectroscopic data and that from electron diffraction (see the introduction section) has now been resolved, as shown in Table 6.

Acknowledgements. One of the authors (K.K.) is grateful to Professors Otto Bastiansen and Yonezo Morino for their stimulating discussions. The present study was initiated under the guidance and strong influence of their brilliant pioneering work around 1960 on the shrinkage effect.

Appendix

The probability distribution function of the bending displacement coordinate ϱ in thermal equilibrium at temperature T is obtained by taking a Bolzmann sum as

$$Q_T(\varrho) = N \sum_{v,l} \exp\left(-\frac{hE'_{vl}}{kT}\right) |\psi'_{vl}(\varrho)|^2, \tag{A1}$$

where E'_{vl} and ψ'_{vl} denote the eigenvalue and the eigenvector of the Hamiltonian, H'_{srb}, defined in eqn. (15) for the v' state, respectively, and N represents a normalizing factor. The radial distribution function for the i-th internuclear distance is calculated by convolution of the Gaussian functions which include all the small-amplitude modes according to[35]

$$P_i(r) = \frac{1}{\sqrt{2\pi}\, l_s(i)} \int_0^\pi Q_T(\varrho) \exp\left[-\frac{(r-r_i(\varrho))^2}{2l_s(i)^2}\right] d\varrho \tag{A2}$$

where $l_s(i)$ is the contribution to the root-mean-square amplitude from all the small-amplitude modes (i.e., all but the ν_7 mode) calculated from the harmonic force constants,[9] and $r_i(\varrho)$ is the i-th distance averaged over all the small-amplitude vibrations. The molecular intensity, $M_i(s)$, for the i-th atomic pair is then calculated from $P_i(r)$ as[14]

$$Mi(s) = \int_0^\infty P_i(r) \frac{\sin(sr)}{sr} dr. \tag{A3}$$

The r_a distance, the mean amplitude, l, and the

asymmetry parameter, $\varkappa$ are estimated by a numerical fitting to $M_i(s)$ according to[14]

$$M_i(s) = \exp\{-\tfrac{1}{2}[l(i)s]^2\}\frac{\sin\{s[r_a(i)-\varkappa(i)s^2]\}}{sr_a(i)} \quad \text{(A4)}$$

The shrinkage, δ_g, is calculated from r_a by using eqn. (1). The total molecular intensity, $M(s)$, is calculated according to

$$M(s) = \sum_i c_i M_i(s), \quad \text{(A5)}$$

where c_i is the coefficient representing the scattering power. This function is fitted to the experimental intensity of electron diffraction.

References

1. Winnewisser, B. P. In: Rao, K. N., Ed., *Molecular Spectroscopy: Modern Research,* Academic Press, New York 1985, Vol. 3, p. 322 and references therein.
2. Almenningen, A., Arnesen, S. P., Bastiansen, O., Seip, H. M. and Seip, R. *Chem. Phys. Lett. 1* (1968) 569.
3. Almenningen, A., Bastiansen, O. and Munthe-Kaas, T. *Acta Chem. Scand. 10* (1956) 261.
4. Almenningen, A., Bastiansen, O. and Traetteberg, M. *Acta Chem. Scand. 13* (1959) 1699.
5. Morino, Y., Nakamura, J. and Moore, P. W. *J. Chem. Phys. 36* (1962) 1050.
6. Tanimoto, M., Kuchitsu, K. and Morino, Y. *Bull. Chem. Soc. Jpn. 43* (1970) 2776.
7. Clark, A. and Seip, H. M. *Chem. Phys. Lett. 6* (1970) 452.
8. Carreira, L. A., Carter, R. O., Durig, J. R., Lord, R. C. and Milionis, C. C. *J. Chem. Phys. 59* (1973) 1028.
9. Duckett, J. A., Mills, I. M. and Robiette, A. G. *J. Mol. Spectrosc. 63* (1976) 249.
10. Fusina, L. and Mills, I. M. *J. Mol. Spectrosc. 79* (1980) 123.
11. Weber, W. H. *J. Mol. Spectrosc. 79* (1980) 396.
12. Bunker, P. R. *J. Mol. Spectrosc. 80* (1980) 422.
13. Egawa, T., Fukuyama, T., Yamamoto, S., Takabayashi, F., Kambara, H., Ueda, T. and Kuchitsu, K. *J. Chem. Phys. 86* (1987) 6018.
14. Kuchitsu, K. and Cyvin, S. J. In: Cyvin, S. J., Ed., *Molecular Structures and Vibrations,* Elsevier, Amsterdam 1972, Chap. 12.
15. Ohshima, Y., Yamamoto, S., Nakata, M. and Kuchitsu, K. *J. Phys. Chem. 91* (1987) 4696.
16. Stock, A. and Stolzenberg, H. *Ber. Dtsch. Chem. Ges. 50* (1917) 498.
17. Miller, F. A. and Fateley, W. G. *Spectrochim. Acta 20* (1964) 253.
18. Murata, Y., Kuchitsu, K. and Kimura, M. *Jpn. J. Appl. Phys. 9* (1970) 591.
19. Yamamoto, S., Nakata, M., Fukuyama, T. and Kuchitsu, K. *J. Phys. Chem. 89* (1985) 3298.
20. Kuchitsu, K., Nakata, M. and Yamamoto, S. In: Hargittai, I., Ed., *Stereochemical Applications of Gas-Phase Electron Diffraction,* VCH, Deerfield Beach, Florida 1988, Chap. 7. *In press.*
21. Kuchitsu, K. *Bull. Chem. Soc. Jpn. 40* (1967) 498.
22. Kuchitsu, K. and Morino, Y. *Bull. Chem. Soc. Jpn. 38* (1965) 805.
23. Bunker, P. R. and Landsberg, B. M. *J. Mol. Spectrosc. 67* (1977) 374.
24. Cooley, J. W. *Math. Comput. 15* (1961) 363.
25. Harris, D. O., Harrington, H. W., Luntz, A. C. and Gwinn, W. D. *J. Chem. Phys. 44* (1966) 3467.
26. Bartell, L. S., Roth, E. A., Hollowell, C. D., Kuchitsu, K. and Young, J. E., Jr. *J. Chem. Phys. 42* (1965) 2683.
27. Sugie, M. *Thesis,* The University of Tokyo, Tokyo 1974.
28. Kato, C., Konaka, S., Iijima, T. and Kimura, M. *Bull. Chem. Soc. Jpn. 42* (1969) 2148.
29. Duncan, J. L. and Mallinson, P. D. *Chem. Phys. Lett. 4* (1973) 597.
30. Pariseau, M. A., Suzuki, H. and Overend, J. *J. Chem. Phys. 42* (1965) 2335.
31. Mallinson, P. D. and Nemes, L. *J. Mol. Spectrosc. 59* (1976) 470.
32. Jensen, H. H., Nilssen, E. W. and Seip, H. M. *Chem. Phys. Lett. 27* (1974) 338.
33. Brown, R. D., Champion, R., Elmes, P. S. and Godfrey, P. D. *J. Am. Chem. Soc. 107* (1985) 4109.
34. Smith, D. F., Jr. and Overend, J. *J. Chem. Phys. 54* (1971) 3632.
35. Karle, J. *J. Chem. Phys. 22* (1954) 1246.

Received March 4, 1988.